

INORGANIC CHEMISTRY FRONTIERS



CHINESE
CHEMICAL
SOCIETY



ROYAL SOCIETY
OF CHEMISTRY

rsc.li/frontiers-inorganic

REVIEW

[View Article Online](#)
[View Journal](#) | [View Issue](#)



Cite this: *Inorg. Chem. Front.*, 2023, **10**, 7095

Received 3rd August 2023,
Accepted 10th October 2023

DOI: 10.1039/d3qi01522j
rsc.li/frontiers-inorganic

Recent advances in electrocatalytic reduction of ambient CO₂ toward high-value feedstock

Naohiro Fujinuma *^a and Samuel E. Lofland *^b

The effects of climate change have arisen due to greenhouse gases emitted into the atmosphere, and the finite supply of fossil fuels will eventually be unable to support the needs of the petrochemical industry. Solutions to these two complex problems will have to be multipronged, but the industrial implementation of the electrocatalytic reduction of CO₂ can help with both issues. Importantly, the demand for multi-carbon feedstock offers immediate financial incentives, accelerating the search for solutions to the climate problem. However, the technology for the electrocatalytic reduction of CO₂ is still in the process of being commercialised, and the use of ambient CO₂ is a prerequisite for widespread adoption. Here we discuss the progress in this area and the remaining barriers to realizing its potential.

1. Introduction

Nature has a rich history of converting CO₂ into valuable resources driven by the abundant renewable energy from the sun. Carbon monoxide dehydrogenase/acetyl-CoA synthase, the main enzymatic complex in thousands of types of bacteria, has been remarkably effective in microorganisms for more than 3.5 billion years, fixing CO₂ as a carbon resource.¹ In contrast, human beings have only enjoyed highly energy-intensive modern life since the industrial revolution, powered by oxidising energetically compressed fossil fuels. This process results in the reverse carbon flow from underground to the atmosphere. This anthropogenic oxidative carbon consumption accounts for the rise of atmospheric CO₂ levels, as illustrated by the Keeling Curve.² Consequently, the United Nations has declared “a code red for humanity”, warning that the concentration of atmospheric greenhouse gases poses a threat to lives, economies, health and food security.

A desired pathway is to aggressively implement renewable energies, which would consequently lead to a dramatic shift in the material production scheme from the fossil-fuel dependent supply chain to one that relies on more sustainable resources. The CO₂ reduction reaction (CO₂RR) has the potential to play a pivotal role in accelerating such a material evolution due to its attractive natural features: it occurs under atmospheric reaction conditions, does not require any side reactants such as hydrogen, is compatible with renewable energy resources, and offers a wide range of potential products.

A literature search shows that the CO₂RR study dates back as far as the 1950s as a way to produce chemicals.^{3,4} In the 1980s and 90s, comprehensive research was conducted on a variety of metal or molecular catalysts and electrolytes to discuss the selectivity of CO₂RR.⁵⁻⁷ As predicted by Hori,⁷ there has been a significant resurgence in the use of CO₂RR within the research community in recent years, resulting in an increasing number of publications equivalent to Moore’s law (Fig. 1). Despite its long history and the renewed focus on developing efficient and selective electrocatalysts, CO₂RR has not been adopted by conventional chemical industries as a replacement for fossil fuels. This is in contrast to lithium-ion battery technology, which was discovered later but has been widely commercialised with an even steeper rise in the publication rate.

Why has nature successfully implemented ambient CO₂ reduction, while the same achievement has thus far eluded

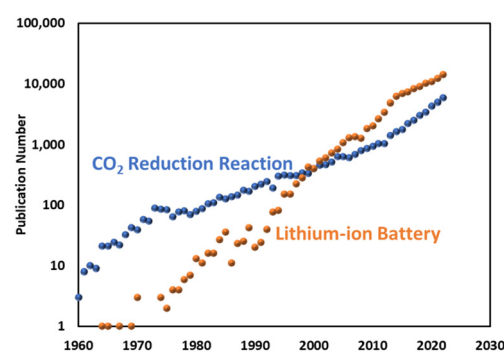


Fig. 1 Annual publications for an electrocatalytic CO₂ reduction reaction and lithium-ion battery research.

^aSekisui Chemical Co., Ltd, 2-4-4 Nishitemma, Kita-ku, Osaka 530-8565, Japan.
E-mail: fujinuma@rowan.edu

^bDepartment of Physics and Astronomy, Rowan University, 201 Mullica Hill Rd., Glassboro, NJ 08028, USA. E-mail: lofland@rowan.edu

human ingenuity? With this question in mind, we will discuss several important aspects of CO₂RR. However, given the breadth of research in this field, this review does not seek to be exhaustive; rather, it aims to provide insight into the economic viability and future of CO₂RR. First, we introduce the potential products of CO₂RR, followed by a techno-economic analysis to shed light on the current barriers towards the successful commercialization of CO₂RR. Finally, we will review a few studies dealing with the less-discussed but significant properties for successful CO₂RR implementation.

2. Basic principles and catalyst science for CO₂RR

One of the attractive but complicating features of CO₂RR is that it has a variety of possible products along with competing hydrogen evolution reaction (HER), all of which have similar standard redox potentials *vs.* reversible hydrogen electrode derived from the Gibbs energy and physicochemical constant.⁸ Due to the close thermodynamic characteristics of CO₂RR, the selectivity of the expected CO₂RR is dependent on both the modulation of electrochemical activation energy toward a specific route and the availability of the corresponding reactants. An electrochemical catalyst is needed to lower the activation energy of a specific target by stabilising an intermediate for the reaction. CO₂RR is an inner-sphere reaction involving multiple electron- and proton-transfer processes. In contrast to an outer-sphere reaction, in which the electron transfer occurs through tunnelling across a monolayer of solvents, the heterogeneous inner-sphere reaction is based on the interaction of a reactant, a product, or an intermediate with the catalyst surface. These interactions enable a critical intermediate species more likely to be structurally changed in subsequent steps.

As a principle, the rate of the multi-step reaction is determined by the slowest step, *i.e.*, the rate-determining step (RDS). It has been proposed that two-electron transfer reactions of CO₂RR into CO or HCOOH may possess different types of RDS.^{9–11}

As for CO₂RR into CO and HCOOH (Fig. 2), steps 1 and 5 represent the CO₂ adsorption process which triggers the CO₂RR pathway. A recent study indicates that this process can be dependent on the applied potential because of the inter-

action between the dipoles of the participating reaction intermediates with the interfacial field.^{10,11} Both field-dependent density functional theory and pH-dependent activity measurements concluded that the ideal catalyst should possess large adsorbate dipoles on CO₂*.¹⁰ Steps 2 and 6 are concerted proton-electron transfer steps, and the configuration of CO₂* seems to determine the selectivity with transition metal surfaces.¹² One computational study¹³ suggests that the C-atom bonding structure leads to the CO production pathway while an O-atom mediated bond is more likely to induce formate/formic acid production. Experimental studies such as *in situ* surface Raman scattering confirm that such a configurational change determines the selectivity of the CO₂RR product.^{14,15} Steps 1' and 5' are proton-decoupled electron-transfer steps whose kinetics are independent of the number of local protons in the vicinity of the catalytic site, followed by the protonation to form COOH or OCOH [steps 2' and 6']. The final step of CO₂RR is the desorption of a product from the catalytic site [steps 4 and 8]. Since the electrochemical activation energy expectedly correlates with the adsorption energy between the intermediate species of the rate determining step and the catalytic sites, the free energy of the adsorption of the intermediate is usually discussed to elucidate the catalyst selectivity.

3. Techno-economic analysis of CO₂RR in the context of performance matrices

Since CO₂RR is an alternative way to produce existing fossil fuel-derived catalysts, the electro-synthesized product needs to compete economically with the widely-established market products. In this context, a techno-economic analysis (TEA) should be considered and included in the discussion of studies which investigate the application of CO₂RR. One of the simplest ways to approximate the economic validity of CO₂RR products is to plot the relationship between the minimum energy requirement for the targeted product and the corresponding market price. Here the minimum energy consumption per unit mass E_{\min} is defined by

$$E_{\min} = n(E_{\text{red}}^{\circ} - E_{\text{min}}^{\circ})F/\text{MW} \quad (1)$$

where n is the electron number for a specific reaction, E_{red}° is the standard redox potential for CO₂RR, E_{ox}° is the standard redox potential for the counter reaction, F is the faradaic constant, and MW is the molar mass of the product.

The thermodynamic cell potential serves as an indicator of the minimum energy requirement for a given product and thus, given the energy costs, provides a means to estimate the economic viability of a product. Fig. 3 shows the possible CO₂RR products plotted as a function of E_{\min} and market price as of 2023. One notices that CO and formic acid are well positioned in this proximity of economic analysis due to its two-electron transfer characteristics. Some oxygenates such as acetic acid and acetaldehyde also possess a relatively high

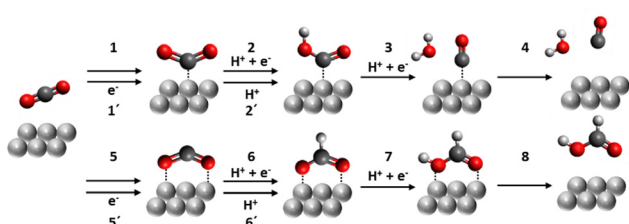


Fig. 2 Reaction schemes for the CO₂ reduction reaction into CO or HCOO.

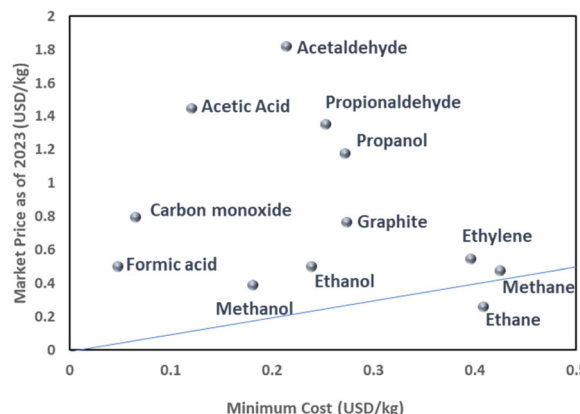


Fig. 3 Possible electrocatalytic CO_2 reduction reaction products plotted as a function of minimum energy consumption per unit mass and market price as of 2023. The line represents the break-even point assuming no additional financial incentives.

market value compared to the required minimum cost. Alcohol derivatives and graphite materials are in the middle group because of the moderate minimum costs and current economic value. As the carbon number in the alcohol increases, the minimum cost and current market price increase concomitantly, indicating that the market price reflects the energy required for the chemical supply. The graph also highlights the challenges of synthesizing hydrocarbon products such as ethylene, methane, and ethane. The discrepancy between the low market price and the high-cost characteristics of these derivatives is attributed to the fundamental differences between the processes in the existing petrochemical infrastructure and in a future CO_2 -based electrochemical supply. Specifically, hydrocarbons can be extracted from fossil fuels without additional energy to convert chemical structures since nature has already converted CO_2 into hydrocarbons over a long period of time. By contrast, CO_2RR needs additional energy to convert CO_2 into hydrocarbons, which inevitably adds costs relative to fossil-fuel-derived hydrocarbons. Since hydrocarbons are a fundamental commodity for the chemical industry, subsidies are likely needed for the timely implementation of CO_2RR to support the hydrocarbon chemical chain.

Note that recent electrocatalyst and photocatalyst studies have demonstrated the combination of CO_2RR and an unconventional anode reaction to either reduce the cell voltage¹⁶ or directly synthesize more complex chemicals,^{17,18} which may pave the way toward an efficient CO_2RR production system.

While the minimum cost approximation is helpful to identify the economic potential of CO_2RR targets, the actual TEA should be more in-depth. There are three basic process steps for CO_2RR : CO_2 purification, CO_2 conversion, and product purification (Fig. 4). The TEA of the overall chemical process reminds us of what we need to rapidly scale up the CO_2RR and, in turn, provides key insights for essential future studies.

The cost associated with CO_2 purification depends on the CO_2 ratio of the initial gas mixture and a capture method. CO_2 captured from concentrated CO_2 sources, such as power and

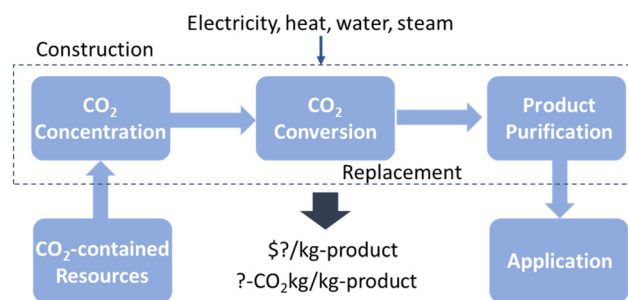


Fig. 4 Basic processes for a scaled-up electrocatalytic CO_2 reduction reaction: CO_2 purification, CO_2 conversion, and product purification.

chemical plants or from amine technology, has the lowest price of $\$50\text{--}70\text{ t}^{-1}$ with a US Department of Energy target of $\$40\text{ t}^{-1}$.¹⁹ On the contrary, capturing CO_2 from the air is more expensive than from flue gas because of its low concentration: one study estimated that the cost for CO_2 capture from the air could potentially reach $\approx\$100\text{--}200\text{ t}^{-1}$ in the future.²⁰ The cost of CO_2 purification in a typical carbon conversion unit provides an opportunity to pursue new technology to simplify or eliminate CO_2 purification. If effluent gas is converted in the CO_2 conversion unit on site in places such as fired power plants or incineration plants, the cost for the CO_2 purification step decreases. In addition, the degree of required CO_2 purification depends on how sensitive the CO_2 conversion is to the impurities in the gas stream entering the CO_2 conversion. For instance, NO_x and SO_x are usually present in exhaust gas and the effects of these oxide impurities on the selectivity and durability of the CO_2RR catalyst are still largely unexplored.

The CO_2RR product purification process includes gas and/or liquid separation, depending on the physicochemical properties of the production. Gas separation is usually required because of the presence of unconverted CO_2 and unintended side products such as H_2 in the product effluent. Liquid product separation is often required to extract products in the liquid catholyte. Pressure swing adsorption (PSA) and membrane technologies are currently used in other industrial processes with similar gas compositions.²¹ It appears that PSA is generally preferred because of its relatively low operating costs and high efficiency with an estimated cost of around $\$10\text{ t}^{-1}$ based on CO_2RR TEA²² and the Sherwood plot for the separation of dilute streams.²³ Liquid product separation can be executed through distillation, extraction, precipitation, and pervaporation.²¹ Among these, distillation is widely used but it is expected to have a much higher operational cost than gas separation with PSA.

The operational cost of the CO_2RR product depends on the purity of the target and chemical composition in the product stream from the electrochemical conversion unit. Thus, both the selectivity and conversion ratio of CO_2RR are imperative to determine the energy required for the purification process. In addition, the additives for the electrochemical reaction, such as electrolyte salts and co-catalysts, should be considered in the cost analysis for the product separation process.

The CO₂ conversion unit operates predominantly with electricity as input energy and CO₂ as feedstock. Therefore, the energy efficiency in converting CO₂ into target chemicals, defined as the ratio of thermodynamic energy to input energy, affects the operational cost of CO₂RR. Energy efficiency is a function of the sum of the overpotential of cathodic and anodic reactions along with other voltage drops in an electrolyser and FE for the specific product. CO₂RR into hydrocarbon such as ethylene usually requires prominent overpotential to kinetically drive the reaction, which may push up the operational costs. As for the CO₂ feedstock, the conversion ratio of CO₂ as a system affects the operational cost as the unconverted CO₂ is either wasted or requires more energy to be recycled. The CO₂RR cell is preferably designed to minimize CO₂ loss. For instance, when an alkaline electrolyte is used on the cathode side, CO₂ loss likely occurs as a dissolved carbonate, preventing the efficient utilization of CO₂. One strategy is to utilize a fully carbonated system with an anion exchange membrane, which leads to the consumption of CO₂ at the cathode and the re-emission of CO₂ with oxygen at a locally acidic anode. However, an additional separation step is required to recover CO₂ from the anode vapours.

As for the capital cost, the partial current density, the observed current for the relevant reaction per geometric area, is important to determine the total electrode size of the electrolyser for the CO₂RR. Given that the number of electrons to be transferred varies depending on the CO₂RR reaction, a more practical manner to evaluate the productivity of CO₂RR may be to convert current density into the production rate of the targeted product per geometric area.

The durability of the CO₂ converting unit or electrochemical cell is also an important factor in affecting the frequency of cell replacement and the operational cost. TEA studies often use a lifecycle of 5–30 years.^{22,24,25} However, conventional CO₂RR studies usually report durability results for times of 10–100 h, and there is a gap between the current testing period and the prolonged durability test required before building the actual plant. Moreover, an accelerated testing protocol needs to be designed to speed up the durability development, which is also currently not well addressed. The definition of the reduction in performance at which the CO₂RR cell should be replaced will remain an open question until key stability/durability relationships are experimentally established.

One should note that the CO₂RR process can reduce or increase CO₂ emissions depending on the energy required for the total production process and the carbon intensity of the electricity and utilization. The carbon intensity of renewable energy is significantly lower than that of fossil fuel-derived electricity, suggesting the combination of the CO₂RR process and such renewable energy can be a more carbon-neutral scheme. In this case, integrating the CO₂RR process into the off-grid renewable energy should be discussed since the plant system requires additional electric equipment, such as energy storage systems and converters. A hydrogen production electrolyser plant powered by renewable energy can be a good model for estimating the cost impact of electricity management in a CO₂RR plant.

The source of CO₂ and electricity significantly affects the cost of the CO₂RR process and the benefit of CO₂ emission reduction. The CO₂RR process prefers more concentrated CO₂ sources in the fluent gas. However, we should envision the long-term viability of CO₂ emitters since the social system will require a change toward more carbon-neutral structures. The electricity price changes significantly depending on the region, the electricity resources, and geopolitical environments. Since the CO₂RR plant is an electricity-demanding process, one needs to choose the place to develop the plant carefully. Usually, TEA applies an electricity cost of 0.02–0.03 USD per kW per h,^{22,24,25} which still limits the actual short-term option to scale up the CO₂RR process, which can reflect the cost simulation of the TEA.

After providing an overview of TEA, we propose emphasizing the following domains in the plant flow (CO₂ concentration, conversion, and the production purification step) for scaling up CO₂RR deployment (Fig. 5): (1) the effect of chemical composition of the feed gas, (2) the industrially relevant productivity and durability of CO₂RR, and (3) maximizing the CO₂ conversion ratio and optimizing selectivity to minimize the need for purification processes.

4. Noteworthy CO₂RR research toward economically valuable feedstock

4.1. Effect of the chemical composition of feed gas

Most CO₂RR research has been carried out with concentrated CO₂, which helps increase the reaction rate and selectivity of CO₂RR due to the high availability of CO₂ at catalytic sites and avoids undesirable side reactions stemming from impurities. As mentioned in section 3, the CO₂ concentration process, while relatively mature, introduces additional energy consumption and costs to implement CO₂RR, which may induce unfavourable CO₂ emissions. Therefore, it is desirable that the CO₂RR is compatible with direct effluents from CO₂ sources. The CO₂ concentration of fired power plants is around 15% (v/v), depending on the type of fossil fuels and combustion

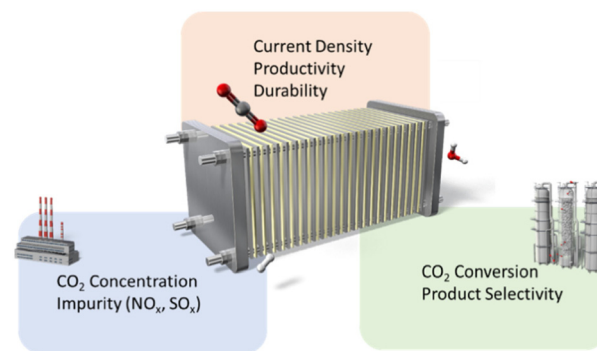


Fig. 5 The highlighted research domain in the process flow of the electrocatalytic CO₂ reduction reaction.

system. Also, industry exhaust streams often contain other gaseous species such as N_2 , O_2 , H_2O , NO_x , SO_x , and volatile organic compounds. The oxidized components of flue gas, such as SO_x and NO_x , may influence CO_2 RR catalysts, although their concentrations are low (typically in the order of hundreds of ppm). Therefore, deviating from pure CO_2 gas could impact the CO_2 RR catalytic activity and durability.

The decrease in CO_2 partial pressure is expected to decrease the reaction rate of CO_2 RR when CO_2 diffusion is a rate-limiting step. This is the case for electrolysis under the practical conditions of operating close to the maximum partial current density regardless of the structure of the electrolyser cell. Additionally, the decreased CO_2 partial pressure creates a reaction environment preferable to the competing HER since the number of protons for the reaction is independent of the gas component. Moreover, the adverse effect of limited CO_2 in the incoming gas may become more severe as the size of the electrolyser increases because the consumption of CO_2 in the gas or electrolyte occurs along with the plane of the electrode, and the gas/liquid stream close to the outlet of the flow cell has the lowest amount of CO_2 . Therefore, the influence of CO_2 partial pressure is a vital factor in determining the compatibility of CO_2 RR with the exhaust gas.

There have been some studies on the effect of CO_2 partial pressure and presenting engineering-based strategies to tackle limitations. Among the pioneering studies in the 1990s,^{26,27} Komatsu observed that the current density and FE for CO_2 RR decreased as CO_2 concentration decreased from 100 to 14% with the copper composite electrode for the gas-phase CO_2 RR.²⁸ Consistent with that work, Kenis *et al.*²⁹ reported that the partial current density noticeably decreased with the decrease in the CO_2 concentration with Ag nanoparticle catalysts on the gas diffusion electrode in the CO_2/N_2 mixture feed in 1 M KCl electrolyte media. The authors also observed the decrease in the FE for CO_2 RR to CO by using phosphate buffer as the electrolyte to distinguish between the effect of CO_2 partial pressure and pH in the electrolyte. The pH dependency study showed that the FE for CO_2 RR to CO decreased more severely with the decrease in pH, suggesting that the number of local protons initiates the HER, diminishing CO_2 RR more easily as either the CO_2 concentration in the feed or the pH in the electrolyte decreased.

A straightforward way to address the diluted CO_2 concentration is to elevate the pressure of the electrolyser system, which increases CO_2 availability at the catalyst. Xu *et al.*³⁰ demonstrated that the pressurization of the feed gas at 15 bar successfully maintained a 91% FE for CO_2 RR to CO with 15% (v/v) CO_2 , which is similar to or higher than that of the performance with pure CO_2 at 1 bar, depending on the applied potential. While pressurization requires some additional energy input, they calculated that the energy required to pressurize to 10 bar represents only ~3% of the energy required to perform efficient CO_2 RR to C_2 products. These results indicate that pressurization helps enable the direct conversion of streams with CO_2 concentrations characteristic of major flue gas sources at industrially relevant current densities.

O_2 is the highest concentration reactive impurity in flue gas and is challenging to remove. The oxygen reduction reaction has a more favourable thermodynamic potential and kinetics compared to CO_2 RR, which significantly impedes the target selectivity. As an initial study, Morikawa *et al.*³¹ confirmed that the inclusion of O_2 significantly reduces the FE for CO_2 RR to formate with a porous ruthenium complex polymer catalyst on a photocathode from 93% (at 0% O_2) to 6% (at 7% O_2) due to the selective O_2 reduction competing with CO_2 reduction. They demonstrated that the combination of the catalyst with carbon papers mitigated the drop of FE to 75% at 7% O_2 , which is attributed to the affinity of the carbon materials to gaseous CO_2 in aqueous solution, resulting in the relatively concentrated CO_2 in the vicinity of the catalytic sites. However, the measurement of local CO_2 should be carried out for further discussion.

Exploiting the difference in solubility between CO_2 and O_2 in the electrolyte media is one way of mitigating the parasitic effect of O_2 . Sinton *et al.*³⁰ exploited an ionomer and TiO_2 coating to create a hydrophilic environment around the Cu catalysts so that CO_2 can predominantly dissolve and reach the catalytic sites over O_2 . They observed a FE towards C_2 products of 68% and energy efficiency of 26% over 10 h of stable operation (at 10 bar), a performance competitive with some of the best results previously reported on reactors using pure CO_2 .

Another methodology to circumvent the oxygen reduction reaction is to implement an additional layer to selectively transport or adsorb CO_2 over O_2 . Wang *et al.*³² demonstrated that a polymer of intrinsic microporosity serves a role in selectively permitting CO_2 to permeate while preventing O_2 from reaching the catalytic sites. They coated the gas separation polymer on the opposite side of the carbon paper of the cobalt phthalocyanine catalyst and observed FE for CO of 75.9% in a gas with 5% O_2 in contrast to the catalyst without the gas separation layer performing no observable FE with the same O_2 concentration. Subsequently,³³ the authors applied aniline molecules to enhance the ability of the permeable ionic membrane (PIM) to separate CO_2 from O_2 using chemical interactions between the acidic CO_2 and the basic amino group of aniline. In an electrolytic flow cell with a cobalt phthalocyanine/carbon nanotube catalyst, they observed a FE for CO of 71% in the presence of 10% O_2 in CO_2 using the PIM/aniline membrane, therefore outperforming the pure PIM with a FE for CO of 63% under the same conditions. While these studies highlight the effectiveness of structurally or chemically engineering the microstructure, further research regarding the physicochemical properties of CO_2 and O combined with kinetic modelling will lead to clearer design principles for selective CO_2 supply in a microenvironment.

NO_x is among the major contaminants present in industrial CO_2 point sources with a typical concentration of 10–500 ppm depending on the regional regulation and combustion system.³⁴ NO_x usually consists of 90–95% NO and 5–10% NO_2 , N_2O being a common by-product formed in the NO_x removal process. All of these NO_x gases can compete with CO_2 for electrons through the corresponding reduction reaction, which

has a more favourable standard redox potential than CO₂RR. Therefore, the kinetics of the NO_x reduction reaction, along with the concentration of NO_x, could be crucial factors to be investigated. Moreover, NO₂ can also react with water to produce various acidic products, including nitric and nitrous acids.

Komatsu *et al.*²⁸ found no effect of 200 ppm NO on the catalytic activity of gas-phase CO₂RR with a copper-deposited electrode. The author argued that the amount of NO was about two times higher than that of the exhaust gas from a typical coal-fired power plant. Jiao *et al.*³⁵ demonstrated that the presence of much higher amounts of NO, NO₂, and N₂O (8300 ppm) in the CO₂ feed leads to a considerable FE loss in CO₂RR with Cu, Ag, and Sn catalyst-loaded gas diffusion electrodes. Notably, they observed the recovery of the FE for CO₂RR after switching the feed gas without NO_x, suggesting that NO_x is involved in the electroreduction process but does not affect the structure of the catalysts in these conditions. In addition, they evaluated the effect of 830 ppm and 83 ppm NO, showing less severe (less than 5%) and negligible losses in FE, respectively, highlighting that CO₂RR can be compatible with typical concentrations of NO_x in flue gases. Note that the parasitic effect of NO_x is dependent on the nature of the catalyst and an electrochemical setup. Oh *et al.*³⁶ reported a decrease in FE for HCOO⁻ from 69.4% to 37.7% using SnS_x as the catalyst in the presence of 90 ppm NO. Sridhar *et al.*³⁷ observed a loss in FE for ethylene of 22.9% after exposing the copper catalyst to 1% NO₂ and a change in the surface colour of the copper catalyst, showing that excessive NO₂ may contribute to the oxidation of the catalysts.

SO_x is another possible chemical component in the gas feed. Typical power plants emit exhaust containing 10–300 ppm SO₂. Komatsu *et al.*²⁸ found that 170 ppm SO₂ in the feed noticeably changed the distribution of the products with a copper catalyst. Jiao *et al.* observed a general decrease in the FE for total CO₂ reduction after copper, silver, and tin catalysts were exposed to a gas stream of 1% SO₂ in CO₂, which is attributed to the preferential reduction of SO₂. Silver and tin catalysts showed less change in the product distribution and the recovery of FE for each product was attained after stopping the feed of SO₂. However, the catalyst characterization shows the sulfurization and desulfurization reaction of Ag and Sn after the SO₂ and pure CO₂ feed, respectively, inferring that these materials are relatively durable against the sulfur-derived structural change. On the contrary, the exposure of SO₂ causes the product distribution with Cu catalysts toward formate, which is irreversible even after switching back to a pure CO₂ stream. The authors attributed the change to residual Cu₂S formed on the surface.

One finds that there is a sizeable difference between the amount of impurities used for the CO₂RR studies mentioned above and the actual content found in the exhaust from specific CO₂ sources. This is because the emitters have often already modified the fraction of impurities to prevent air pollution. Therefore, in more practical scenarios, the tested chemical composition for CO₂RR needs to match the actual

composition for a true feasibility study. Investigations into the effects of impurities on the durability of the CO₂RR catalyst should also be conducted. Since the existing CO₂ purification process, such as the amine adsorption method, already works to reduce the impurities, the total design of combining the CO₂ purification and conversion relies on the efficiency and durability of the CO₂RR process.

Current CO₂RR demands a high CO₂ partial pressure compared to nature, which converts 440 ppm CO₂ with highly diluted solar energy. While direct air capture is in the pilot phase of plant testing, the general cost for concentrating CO₂ from a level of a few hundred ppm to nearly 100% is unacceptably high due to the intensive energy required for the process. One option would be combining the CO₂ concentrator and a converter compatible with significantly diluted CO₂ sources, but resolving the issues surrounding gas impurities needs to be addressed first.

4.2. Industrially relevant productivity and durability of CO₂RR

While the FE and energy efficiency for a specific product affect the operational cost of electrolysis, the current density or productivity per geometric surface area of the electrode is essential in determining the capital cost since as the productivity increases, the size of the electrolyser decreases. The current density is typically one of the matrices used to evaluate CO₂RR research. A practical measure is the productivity of the specific product per specific time and the electrode geometric area.

Fig. 6a shows the reported partial current density and expected production rate per day for various products.^{33–126} HCOOH/HOO⁻ has the highest value of production rate per partial current density due to its 2-electron transfer characteristics and relatively high molecular weight, followed by CO production. CO₂ to ethanol or ethylene has a lower production rate per partial current density because these products require 12 electrons to be transferred to the reactant but have a similar molecular weight.

Significant efforts to improve the partial current density have been made in the last few years, mainly focusing on the catalyst design to increase the catalytic site density and electrochemical cell engineering to achieve gas-phase reactions to cir-

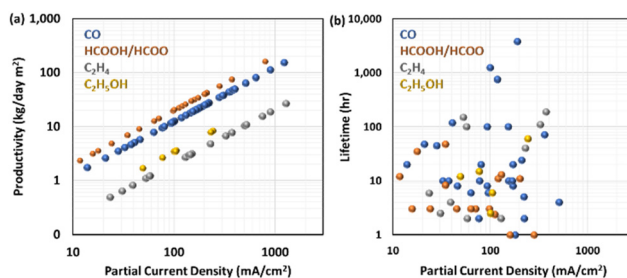


Fig. 6 (a) The expected production rate per day as a function of the partial current density for each CO₂RR product with the experimental data according to the literature survey. (b) Reported lifetime of CO₂RR as a function of the partial current density for each CO₂RR product with the experimental data according to the literature survey.

cumvent the limitations of CO_2 solubility in the electrolyte. The flow or membrane electrode assembly (MEA) cell configuration with a gas diffusion electrode especially has played a central role in creating a three-phase boundary environment where CO_2 can encounter the catalytic sites and ions as a counterpart for the CO_2RR reaction. In addition, recent studies¹²⁷ have introduced micropores or a hydrophobic environment in the catalytic layer to accumulate CO_2 near the catalytic sites.

Sun *et al.*¹²⁸ demonstrated a hierarchical nanoporous catalyst by retaining the micropores of a metal-organic framework precursor to enhance CO_2 concentration in the gas-diffusion electrode, achieving 645 mA cm^{-2} CO partial current density at -0.53 V *vs.* RHE with 86% FE for CO under ambient conditions, which is equivalent to a production rate of $80 \text{ kg d}^{-1} \text{ m}^{-2}$. Chen *et al.*⁷⁸ developed a cell with 450 mA cm^{-2} partial current density with 90% FE for formate with a SnO_2 electrocatalyst. This corresponds to an impressive production rate of $88 \text{ kg d}^{-1} \text{ m}^{-2}$. Liao *et al.*¹²⁹ implemented a Ni-N₅-C single atom catalyst in a flow cell configuration, achieving industrial-scale performance for CO_2RR to CO a FE of 97% at a current density reaching a maximum of 1.23 A cm^{-2} with an FE of 99.6%, the highest production rate of CO_2RR to CO of $154 \text{ kg d}^{-1} \text{ m}^{-2}$ to date. The authors attributed the high performance to the Ni-N₅ catalytic site, which is superior in activating CO_2 molecules and reducing the energy barriers for the intermediate binding energy for boosting the kinetic activation process and catalytic activity. Endrődi *et al.* employed a PiperION membrane for electrocatalytic CO_2 reduction to CO in a tailored zero-gap electrolyser.¹³⁰ This membrane possesses high carbonate-ion conductivity, leading to a high CO current density (over 1 A cm^{-2}) with commercial Ag nanoparticles while maintaining a high FE for CO (up to 90%).

In contrast to the recent rapid advancement of the productivity of CO_2RR , industrially relevant durability has not been achieved yet. Many durability tests (Fig. 6b), including the aforementioned industrially viable production rates, are in the range of 10–100 h. There are only a few studies on CO_2RR to CO that report durability test results over 1000 h long. Notably, one case⁴⁴ involves a commercially available anion-exchange membrane (Sustainion) incorporated in MEAs, which illustrated at least 3800 hours of activity at 190 mA cm^{-2} with FE for CO_2RR to CO of 95% with a silver nanoparticle cathode and an IrO_x anode. The authors implemented two strategies to keep the membrane hydrated: (1) humidifying CO_2 and (2) circulating deionized water or diluted KHCO_3 solution in the anode.

In general, more thorough durability testing is required. So far, only *ex situ* and after-use characterization has been carried out for the CO_2RR electrolyser. There is an urgent need to develop conditions for accelerated testing and then correlating the results between accelerated aging and actual performance.

4.3. Minimizing the purification process

Here we suggest distinguishing between two performance metrics regarding the CO_2RR conversion. One is the CO_2 con-

version efficiency (CE_{CO_2}) defined as the ratio of the amount of CO_2 converted into a target to the amount of CO_2 fed into the system. Another important but less discussed factor is product selectivity, defined as the fractional amount of the target product within the total stream. The former is relevant to the cost of CO_2 consumption and recovery if necessary, and there are some recent studies focused on CE_{CO_2} . The latter is important to determine how much energy is needed to purify the product in the following chemical process. The electrochemical cell can be divided into the cathode and anode compartments, and a path for the product stream is not always the same as the CO_2 flow pathway since the CO_2 can cross the membrane; CE_{CO_2} is often independent of the product selectivity.

Most CO_2RR studies have been carried out in neutral and alkaline electrolytes to impede HER, in which the high current density often creates a strongly alkaline microenvironment at the cathodic interface. This consumes some CO_2 in the feed through sequential chemical reactions of CO_2 driven by the pH gradient in the cell.^{66,132,133} Specifically, an unfavourable reaction between CO_2 and OH^- produces carbonate or bicarbonate, which subsequently crosses the anion exchange membrane to the anode, reacts with H^+ from the oxygen evolution reaction, and is converted to CO_2 in the anode tail gas, giving rise to a low theoretical single pass conversion rate of 50%. Moreover, bicarbonates precipitate with alkaline metals at the cathode once their local solubility hits the limit, which closes micro-channels for CO_2 and ion for the CO_2RR and causes a degradation mode.¹³⁴ It is expected that regenerating lost CO_2 demands additional energy and operating costs.

One adopted strategy for overcoming the CO_2 carbonation problem is to provide CO_2 regeneration space between the catalytic layer and an ion exchange membrane while maintaining the anionic micro-environment in the vicinity of the catalytic site. This methodology has been implemented by including additives in the catalyst layer or inserting an additional buffer layer.^{124,135,136}

O'Brien *et al.*¹³⁵ developed a permeable CO_2 regeneration layer, which provides an alkaline environment at the CO_2RR catalyst surface and enables local CO_2 regeneration concomitantly. They coated the copper cathode layer with the functional groups of the anion exchange polymer (Aemion AP1-CNN5-00-X) to create a positive space charge, enabling the transport of anions and impeding the cations. The polymer coating on the cathode allows for CO_2 transport to the catalyst *via* diffusion through the water-filled hydrated ionic domains in the polymer matrix. With the careful tuning of the thickness of the regeneration layer of $\sim 10 \mu\text{m}$ to minimize impedance to CO_2 and water, they attained 85% CE_{CO_2} with a cation exchange membrane (Nafion 117) and deionized water. The authors proposed that the positively charged functional groups in the polymer structure act as a positive charge as an alternative to alkali metal cations, which can stabilize CO_2RR intermediates to promote C-C coupling on copper catalysts.

Li *et al.*¹³⁶ demonstrated that an acid-fed MEA for CO_2 electroreduction to CO with an H^+ to Cs^+ satisfies both the FE and

conversion efficiency of CO₂. Essentially, an anion-exchange ionomer with quaternary ammonium side chains was incorporated into the Ag catalyst layer to shield the Ag surface from a high proton flux and provide diffusion pathways for dissolved CO₂ and water. After optimizing ion concentrations and operation parameters, they observed a single-pass conversion efficiency of ~90% and long-term stability of 50 h.

While such device and process engineering is an attractive approach, the carbonation of CO₂ at a microscopic level, which seems inevitable as long as the local environment is basic, and the subsequent regeneration process across the two components raise concerns about the long-term durability of the cycle. Moreover, the use of alkaline metals raises another issue of metal precipitation.^{137,138} Therefore, designing a catalyst to accomplish acidic CO₂RR without alkaline metals is an imperative subject for tackling both the CO₂ conversion ratio and precipitation problem. One alternative is a metal-heteroatom-involved polymer catalyst, which is compatible with zero-gap CEM cells with deionized water.¹³¹ Such a configuration may contribute to increasing the CO₂ conversion efficiency.

The product selectivity of CO₂RR is less discussed in most CO₂RR studies, though the plant process design requires the specification of the product component from the conversion unit to access the cost of the following purification. Krause *et al.*¹³⁹ reported the product gas composition in an effort to scale up the CO₂RR to CO. The ratio of CO₂ in the product gas was 10–50% which significantly depends on the CO₂ flow rate and current density. Since product selectivity is closely linked to operation and structural parameters, it is important to clarify both CO₂ conversion efficiency and product concentration, especially when the CO₂RR is scaled up.

There have been several recent approaches to engineer selectivity. Rather than a constant potential for electrosynthesis, Timoshenko and colleagues¹⁴⁰ have used electrical pulses to tune the products. This presumably protects the catalyst from poisoning. Liu *et al.*¹⁴¹ developed pyramidal catalysts, the shape of which presumably controlled the selectivity. While such effects, such as confinement, have long been known, Zhu *et al.*¹⁴² used multilayer pyramids to optimize selectivity by combining geometrical effects with layer sequencing to accelerate the reaction. To reach the requisite selectivity, such synergies in the catalyst (and even electrolyser) design must be exploited.

5. Conclusions

For CO₂RR to be rapidly implemented, it must be scalable and profitable, providing the means and incentive for the procedure. Scalability requires readily available catalysts, electrolytes, and devices that can safely operate with ambient CO₂. On the other hand, profitability necessitates affordable and durable electrolyzers that synthesize value-added products with energy efficient processes at a sufficiently high rate and purity. While nature has had billions of years to perfect photosynthesis, our first intentional use of catalysts for any type of

synthesis can be traced back to just over a century ago, and our efforts on CO₂RR are even more recent. Nevertheless, our knowledge has grown rapidly. This acceleration can be attributed to continued progress in experimental techniques with the advent of *in operando* measurements to verify the reaction mechanisms, the understanding and development of quantum chemistry to provide the theoretical framework, and now the use of artificial intelligence to examine trends to fill the gaps between experimental results and computational predictions in this multi-dimensional space. Discovery has been advanced by high throughput investigations, yet the promise of CO₂RR has yet to be realized on an industrial scale especially with perhaps the most important outstanding issues – purity and durability. Given the progress that humanity has made in the exceedingly short time spent investigating viable CO₂RR, in comparison to the eons nature has had to perfect the process, it is not a question of if we succeed in its realization but when.

Author contributions

Naohiro Fujinuma: Writing – original draft, writing – review & editing; Samuel Lofland: Conceptualization, writing – review & editing, funding acquisition.

Conflicts of interest

There are no conflicts to declare.

Acknowledgements

SEL acknowledges support from Sekisui Chemical Ltd.

References

- 1 P. S. Adam, G. Borrel and S. Gribaldo, Evolutionary history of carbon monoxide dehydrogenase/acetyl-CoA synthase, one of the oldest enzymatic complexes, *Proc. Natl. Acad. Sci. U. S. A.*, 2018, **115**, E1166–E1173.
- 2 D. C. Harris, Charles David keeling and the story of atmospheric CO₂ measurements, *Anal. Chem.*, 2010, **82**, 7865–7870.
- 3 J. Giner, Electrochemical reduction of CO₂ on platinum electrodes in acid solutions, *Electrochim. Acta*, 1963, **8**, 857–865.
- 4 T. E. Teeter and P. Van Rysselberghe, Reduction of Carbon Dioxide on Mercury Cathodes, *J. Chem. Phys.*, 1954, **22**, 759–760.
- 5 H. Noda, S. Ikeda, Y. Oda, K. Imai, M. Maeda and K. Ito, Electrochemical Reduction of Carbon Dioxide at Various Metal Electrodes in Aqueous Potassium Hydrogen Carbonate Solution, *Bull. Chem. Soc. Jpn.*, 1990, **63**, 2459–2462.

6 N. Furuya and K. Matsui, Electroreduction of carbon dioxide on gas-diffusion electrodes modified by metal phthalocyanines, *J. Electroanal. Chem. Interfacial Electrochem.*, 1989, **271**, 181–191.

7 Y. Hori, Electrochemical CO₂ Reduction on Metal Electrodes, *Mod. Aspects Electrochem.*, 2008, 89–189.

8 S. Nitopi, E. Bertheussen, S. B. Scott, X. Liu, A. K. Engstfeld, S. Horch, B. Seger, I. E. L. Stephens, K. Chan, *et al.*, Progress and Perspectives of Electrochemical CO₂ Reduction on Copper in Aqueous Electrolyte, *Chem. Rev.*, 2019, **119**, 7610–7672.

9 M. Dunwell, W. Luc, Y. Yan, F. Jiao and B. Xu, Understanding Surface-Mediated Electrochemical Reactions: CO₂ Reduction and beyond, *ACS Catal.*, 2018, **8**, 8121–8129.

10 S. Vijay, W. Ju, S. Brückner, S. C. Tsang, P. Strasser and K. Chan, Unified mechanistic understanding of CO₂ reduction to CO on transition metal and single atom catalysts, *Nat. Catal.*, 2021, **4**, 1024–1031.

11 J. A. Gauthier, M. Fields, M. Bajdich, L. D. Chen, R. B. Sandberg, K. Chan and J. K. Nørskov, Facile Electron Transfer to CO₂ during Adsorption at the Metal|Solution Interface, *J. Phys. Chem. C*, 2019, **123**, 29278–29283.

12 Y. Y. Birdja, E. Pérez-Gallent, M. C. Figueiredo, A. J. Göttle, F. Calle-Vallejo and M. T. M. Koper, Advances and challenges in understanding the electrocatalytic conversion of carbon dioxide to fuels, *Nat. Energy*, 2019, **4**, 732–745.

13 J. S. Yoo, R. Christensen, T. Vegge, J. K. Nørskov and F. Studt, Theoretical Insight into the Trends that Guide the Electrochemical Reduction of Carbon Dioxide to Formic Acid, *ChemSusChem*, 2016, **9**, 358–363.

14 B. Zhang, Y. Chang, Y. Wu, Z. Fan, P. Zhai, C. Wang, J. Gao, L. Sun and J. Hou, Regulating *OCHO Intermediate as Rate-Determining Step of Defective Oxynitride Nanosheets Enabling Robust CO₂ Electroreduction, *Adv. Energy Mater.*, 2022, **12**, 2200321.

15 J. Chen, B. Ma, Z. Xie, W. Li, Y. Yang, M. Mu, X. Zou, B. Zhao and W. Song, Bifunctional porous SnO₂/Ag nanofibers for efficient electroreduction of carbon dioxide to formate and its mechanism elucidation by *in situ* surface-enhanced Raman scattering, *Appl. Catal., B*, 2023, **325**, 122350.

16 S. Verma, S. Lu and P. J. A. Kenis, Co-electrolysis of CO₂ and glycerol as a pathway to carbon chemicals with improved technoeconomics due to low electricity consumption, *Nat. Energy*, 2019, **4**, 466–474.

17 C. Han, Y. H. Li, J. Y. Li, M. Y. Qi, Z. R. Tang and Y. J. Xu, Cooperative Syngas Production and C–N Bond Formation in One Photoredox Cycle, *Angew. Chem., Int. Ed.*, 2021, **60**, 7962–7970.

18 L. Yuan, M. Y. Qi, Z. R. Tang and Y. J. Xu, Coupling Strategy for CO₂ Valorization Integrated with Organic Synthesis by Heterogeneous Photocatalysis, *Angew. Chem., Int. Ed.*, 2021, **60**, 21150–21172.

19 SunShot 2030 | Department of Energy, < <https://www.energy.gov/eere/solar/sunshot-2030>> (31 July 2023).

20 A. Raksajati, M. T. Ho and D. E. Wiley, Reducing the cost of CO₂ capture from flue gases using aqueous chemical absorption, *Ind. Eng. Chem. Res.*, 2013, **52**, 16887–16901.

21 J. B. Greenblatt, D. J. Miller, J. W. Ager, F. A. Houle and I. D. Sharp, The Technical and Energetic Challenges of Separating (Photo)Electrochemical Carbon Dioxide Reduction Products, *Joule*, 2018, **2**, 381–420.

22 M. Jouny, W. Luc and F. Jiao, General Techno-Economic Analysis of CO₂ Electrolysis Systems, *Ind. Eng. Chem. Res.*, 2018, **57**, 2165–2177.

23 S. Verma, B. Kim, H. R. M. Jhong, S. Ma and P. J. A. Kenis, A Gross-Margin Model for Defining Technoeconomic Benchmarks in the Electroreduction of CO₂, *ChemSusChem*, 2016, **9**, 1972–1979.

24 P. De Luna, C. Hahn, D. Higgins, S. A. Jaffer, T. F. Jaramillo and E. H. Sargent, What would it take for renewably powered electrosynthesis to displace petrochemical processes?, *Science*, 2019, **364**, eaav3506.

25 J. M. Spurgeon and B. Kumar, A comparative technoeconomic analysis of pathways for commercial electrochemical CO₂ reduction to liquid products, *Energy Environ. Sci.*, 2018, **11**, 1536–1551.

26 G. Z. Kyriacou and A. K. Anagnostopoulos, Influence CO₂ partial pressure and the supporting electrolyte cation on the product distribution in CO₂ electroreduction, *J. Appl. Electrochem.*, 1993, **23**, 483–486.

27 N. Hidetomo, I. Shoichiro, Y. Akio, E. Hisahiko and I. Kaname, Kinetics of Electrochemical Reduction of Carbon Dioxide on a Gold Electrode in Phosphate Buffer Solutions, *Bull. Chem. Soc. Jpn.*, 2006, **68**, 1889–1895.

28 S. Komatsu, M. Tanaka, A. Okumura and A. Kungi, Preparation of Cu-solid polymer electrolyte composite electrodes and application to gas-phase electrochemical reduction of CO₂, *Electrochim. Acta*, 1995, **40**, 745–753.

29 B. Kim, S. Ma, H. R. Molly Jhong and P. J. A. Kenis, Influence of dilute feed and pH on electrochemical reduction of CO₂ to CO on Ag in a continuous flow electrolyzer, *Electrochim. Acta*, 2015, **166**, 271–276.

30 Y. Xu, J. P. Edwards, J. Zhong, C. P. O'Brien, C. M. Gabardo, C. McCallum, J. Li, C. T. Dinh, E. H. Sargent, *et al.*, Oxygen-tolerant electroproduction of C₂ products from simulated flue gas, *Energy Environ. Sci.*, 2020, **13**, 554–561.

31 T. Arai, S. Sato and T. Morikawa, A monolithic device for CO₂ photoreduction to generate liquid organic substances in a single-compartment reactor, *Energy Environ. Sci.*, 2015, **8**, 1998–2002.

32 X. Lu, Z. Jiang, X. Yuan, Y. Wu, R. Malpass-Evans, Y. Zhong, Y. Liang, N. B. McKeown and H. Wang, A bio-inspired O₂-tolerant catalytic CO₂ reduction electrode, *Sci. Bull.*, 2019, **64**, 1890–1895.

33 L. Liao, R. An, H. Li, Y. Xu, J. J. Wu and X. Zhao, Catalytic Access to Functionalized Allylic gem-Difluorides via Fluorinative Meyer-Schuster-Like Rearrangement, *Angew. Chem., Int. Ed.*, 2020, **59**, 11010–11019.

34 8.7. Nitrogen Oxides (NO_x) Emissions | netl.doe.gov, <<https://www.netl.doe.gov/research/Coal/energy-systems/gasification/gasifipedia/nitrogen-oxides>> (31 July 2023).

35 B. H. Ko, B. Hasa, H. Shin, E. Jeng, S. Overa, W. Chen and F. Jiao, The impact of nitrogen oxides on electrochemical carbon dioxide reduction, *Nat. Commun.*, 2020, **11**, 1–9.

36 B. U. Choi, Y. C. Tan, H. Song, K. B. Lee and J. Oh, System Design Considerations for Enhancing Electroproduction of Formate from Simulated Flue Gas, *ACS Sustainable Chem. Eng.*, 2021, **9**, 2348–2357.

37 Y. Zhai, L. Chiachiarelli and N. Sridhar, Effect of Gaseous Impurities on the Electrochemical Reduction of CO_2 on Copper Electrodes, *ECS Trans.*, 2009, **19**, 1–13.

38 D. Kopljarić, N. Wagner and E. Klemm, Transferring Electrochemical CO_2 Reduction from Semi-Batch into Continuous Operation Mode Using Gas Diffusion Electrodes, *Chem. Eng. Technol.*, 2016, **39**, 2042–2050.

39 H. Yang, J. J. Kaczur, S. D. Sajjad and R. I. Masel, Electrochemical conversion of CO_2 to formic acid utilizing Sustainion™ membranes, *J. CO₂ Util.*, 2017, **20**, 208–217.

40 X. Lu, D. Y. C. Leung, H. Wang and J. Xuan, A high performance dual electrolyte microfluidic reactor for the utilization of CO_2 , *Appl. Energy*, 2017, **194**, 549–559.

41 S. Ma, M. Sadakiyo, R. Luo, M. Heima, M. Yamauchi and P. J. A. Kenis, One-step electrosynthesis of ethylene and ethanol from CO_2 in an alkaline electrolyzer, *J. Power Sources*, 2016, **301**, 219–228.

42 C. Reller, R. Krause, E. Volkova, B. Schmid, S. Neubauer, A. Rucki, M. Schuster and G. Schmid, Selective Electroreduction of CO_2 toward Ethylene on Nano Dendritic Copper Catalysts at High Current Density, *Adv. Energy Mater.*, 2017, **7**, 1602114.

43 C. T. Dinh, T. Burdyny, G. Kibria, A. Seifitokaldani, C. M. Gabardo, F. Pelayo García De Arquer, A. Kiani, J. P. Edwards, P. De Luna, *et al.*, CO_2 electroreduction to ethylene via hydroxide-mediated copper catalysis at an abrupt interface, *Science*, 2018, **360**, 783–787.

44 Z. Liu, H. Yang, R. Kutz and R. I. Masel, CO_2 Electrolysis to CO and O_2 at High Selectivity, Stability and Efficiency Using Sustainion Membranes, *J. Electrochem. Soc.*, 2018, **165**, J3371–J3377.

45 J. J. Kaczur, H. Yang, Z. Liu, S. D. Sajjad and R. I. Masel, Carbon dioxide and water electrolysis using new alkaline stable anion membranes, *Front. Chem.*, 2018, **6**, 377597.

46 T. Haas, R. Krause, R. Weber, M. Demler and G. Schmid, Technical photosynthesis involving CO_2 electrolysis and fermentation, *Nat. Catal.*, 2018, **1**, 32–39.

47 S. Verma, Y. Hamasaki, C. Kim, W. Huang, S. Lu, H. R. M. Jhong, A. A. Gewirth, T. Fujigaya, N. Nakashima, *et al.*, Insights into the Low Overpotential Electroreduction of CO_2 to CO on a Supported Gold Catalyst in an Alkaline Flow Electrolyzer, *ACS Energy Lett.*, 2018, **3**, 193–198.

48 C. M. Gabardo, A. Seifitokaldani, J. P. Edwards, C. T. Dinh, T. Burdyny, M. G. Kibria, C. P. O'Brien, E. H. Sargent and D. Sinton, Combined high alkalinity and pressurization enable efficient CO_2 electroreduction to CO, *Energy Environ. Sci.*, 2018, **11**, 2531–2539.

49 K. Jiang, S. Siahrostami, T. Zheng, Y. Hu, S. Hwang, E. Stavitski, Y. Peng, J. Dynes, M. Gangisetty, *et al.*, Isolated Ni single atoms in graphene nanosheets for high-performance CO_2 reduction, *Energy Environ. Sci.*, 2018, **11**, 893–903.

50 X. Lu, Y. Wu, X. Yuan, L. Huang, Z. Wu, J. Xuan, Y. Wang and H. Wang, High-Performance Electrochemical CO_2 Reduction Cells Based on Non-noble Metal Catalysts, *ACS Energy Lett.*, 2018, **3**, 2527–2532.

51 B. Endrődi, E. Kecsenovity, A. Samu, F. Darvas, R. V. Jones, V. Török, A. Danyi and C. Janáky, Multilayer Electrolyzer Stack Converts Carbon Dioxide to Gas Products at High Pressure with High Efficiency, *ACS Energy Lett.*, 2019, **4**, 1770–1777.

52 D. A. Salvatore, D. M. Weekes, J. He, K. E. Dettelbach, Y. C. Li, T. E. Mallouk and C. P. Berlinguette, Electrolysis of Gaseous CO_2 to CO in a Flow Cell with a Bipolar Membrane, *ACS Energy Lett.*, 2018, **3**, 149–154.

53 P. Jeanty, C. Scherer, E. Magori, K. Wiesner-Fleischer, O. Hinrichsen and M. Fleischer, Upscaling and continuous operation of electrochemical CO_2 to CO conversion in aqueous solutions on silver gas diffusion electrodes, *J. CO₂ Util.*, 2018, **24**, 454–462.

54 P. De Luna, R. Quintero-Bermudez, C. T. Dinh, M. B. Ross, O. S. Bushuyev, P. Todorović, T. Regier, S. O. Kelley, P. Yang, *et al.*, Catalyst electro-redeposition controls morphology and oxidation state for selective carbon dioxide reduction, *Nat. Catal.*, 2018, **1**, 103–110.

55 T. T. Zhuang, Z. Q. Liang, A. Seifitokaldani, Y. Li, P. De Luna, T. Burdyny, F. Che, F. Meng, Y. Min, *et al.*, Steering post-C–C coupling selectivity enables high efficiency electroreduction of carbon dioxide to multi-carbon alcohols, *Nat. Catal.*, 2018, **1**, 421–428.

56 M. Luo, Z. Wang, Y. C. Li, J. Li, F. Li, Y. Lum, D. H. Nam, B. Chen, J. Wicks, *et al.*, Hydroxide promotes carbon dioxide electroreduction to ethanol on copper via tuning of adsorbed hydrogen, *Nat. Commun.*, 2019, **10**, 1–7.

57 F. Li, Y. C. Li, Z. Wang, J. Li, D. H. Nam, Y. Lum, M. Luo, X. Wang, A. Ozden, *et al.*, Cooperative CO_2 -to-ethanol conversion via enriched intermediates at molecule–metal catalyst interfaces, *Nat. Catal.*, 2019, **3**, 75–82.

58 F. P. García de Arquer, C. T. Dinh, A. Ozden, J. Wicks, C. McCallum, A. R. Kirmani, D. H. Nam, C. Gabardo, A. Seifitokaldani, *et al.*, CO_2 electrolysis to mult carbon products at activities greater than 1 A cm^{-2} , *Science*, 2020, **367**, 661–666.

59 X. Wang, Z. Wang, F. P. García de Arquer, C. T. Dinh, A. Ozden, Y. C. Li, D. H. Nam, J. Li, Y. S. Liu, *et al.*, Efficient electrically powered CO_2 -to-ethanol via suppression of deoxygenation, *Nat. Energy*, 2020, **5**, 478–486.

60 X. Wang, A. Xu, F. Li, S. F. Hung, D. H. Nam, C. M. Gabardo, Z. Wang, Y. Xu, A. Ozden, *et al.*, Efficient Methane Electrosynthesis Enabled by Tuning Local CO_2 Availability, *J. Am. Chem. Soc.*, 2020, **142**, 3525–3531.

61 Z. Yin, H. Peng, X. Wei, H. Zhou, J. Gong, M. Huai, L. Xiao, G. Wang, J. Lu, *et al.*, An alkaline polymer electrolyte CO_2 electrolyzer operated with pure water, *Energy Environ. Sci.*, 2019, **12**, 2455–2462.

62 W. Lee, Y. E. Kim, M. H. Youn, S. K. Jeong and K. T. Park, Catholyte-Free Electrocatalytic CO_2 Reduction to Formate, *Angew. Chem., Int. Ed.*, 2018, **57**, 6883–6887.

63 J. Lee, J. Lim, C. W. Roh, H. S. Whang and H. Lee, Electrochemical CO_2 reduction using alkaline membrane electrode assembly on various metal electrodes, *J. CO₂ Util.*, 2019, **31**, 244–250.

64 R. Xia, S. Zhang, X. Ma and F. Jiao, Surface-functionalized palladium catalysts for electrochemical CO_2 reduction, *J. Mater. Chem. A*, 2020, **8**, 15884–15890.

65 Q. Gong, P. Ding, M. Xu, X. Zhu, M. Wang, J. Deng, Q. Ma, N. Han, Y. Zhu, *et al.*, Structural defects on converted bismuth oxide nanotubes enable highly active electrocatalysis of carbon dioxide reduction, *Nat. Commun.*, 2019, **10**, 1–10.

66 G. O. Larrazábal, P. Strøm-Hansen, J. P. Heli, K. Zeiter, K. T. Therkildsen, I. Chorkendorff and B. Seger, Analysis of Mass Flows and Membrane Cross-over in CO_2 Reduction at High Current Densities in an MEA-Type Electrolyzer, *ACS Appl. Mater. Interfaces*, 2019, **11**, 41281–41288.

67 T. Möller, W. Ju, A. Bagger, X. Wang, F. Luo, T. Ngo Thanh, A. S. Varela, J. Rossmeisl and P. Strasser, Efficient CO_2 to CO electrolysis on solid Ni–N–C catalysts at industrial current densities, *Energy Environ. Sci.*, 2019, **12**, 640–647.

68 T. Zheng, K. Jiang, N. Ta, Y. Hu, J. Zeng, J. Liu and H. Wang, Large-Scale and Highly Selective CO_2 Electrocatalytic Reduction on Nickel Single-Atom Catalyst, *Joule*, 2019, **3**, 265–278.

69 S. Ren, D. Joulié, D. Salvatore, K. Torbensen, M. Wang, M. Robert and C. P. Berlinguette, Molecular electrocatalysts can mediate fast, selective CO_2 reduction in a flow cell, *Science*, 2019, **365**, 367–369.

70 W. H. Cheng, M. H. Richter, I. Sullivan, D. M. Larson, C. Xiang, B. S. Brunschwig and H. A. Atwater, CO_2 Reduction to CO with 19% Efficiency in a Solar-Driven Gas Diffusion Electrode Flow Cell under Outdoor Solar Illumination, *ACS Energy Lett.*, 2020, 470–476.

71 J. P. Edwards, Y. Xu, C. M. Gabardo, C. T. Dinh, J. Li, Z. B. Qi, A. Ozden, E. H. Sargent and D. Sinton, Efficient electrocatalytic conversion of carbon dioxide in a low-resistance pressurized alkaline electrolyzer, *Appl. Energy*, 2020, **261**, 114305.

72 J. Chen, Z. Wang, H. Lee, J. Mao, C. A. Grimes, C. Liu, M. Zhang, Z. Lu, Y. Chen, *et al.*, Efficient electroreduction of CO_2 to CO by Ag-decorated S-doped g-C₃N₄/CNT nanocomposites at industrial scale current density, *Mater. Today Phys.*, 2020, **12**, 100176.

73 T. Li, E. W. Lees, M. Goldman, D. A. Salvatore, D. M. Weekes and C. P. Berlinguette, Electrolytic Conversion of Bicarbonate into CO in a Flow Cell, *Joule*, 2019, **3**, 1487–1497.

74 Y. C. Li, G. Lee, T. Yuan, Y. Wang, D. H. Nam, Z. Wang, F. P. Garcíá De Arquer, Y. Lum, C. T. Dinh, *et al.*, CO_2 Electroreduction from Carbonate Electrolyte, *ACS Energy Lett.*, 2019, **4**, 1427–1431.

75 C. Xia, P. Zhu, Q. Jiang, Y. Pan, W. Liang, E. Stavitsk, H. N. Alshareef and H. Wang, Continuous production of pure liquid fuel solutions via electrocatalytic CO_2 reduction using solid-electrolyte devices, *Nat. Energy*, 2019, **4**, 776–785.

76 T. Shinagawa, G. O. Larrazábal, A. J. Martín, F. Krumeich and J. Pérez-Ramírez, Sulfur-Modified Copper Catalysts for the Electrochemical Reduction of Carbon Dioxide to Formate, *ACS Catal.*, 2018, **8**, 837–844.

77 S. Sen, S. M. Brown, M. L. Leonard and F. R. Brushett, Electroreduction of carbon dioxide to formate at high current densities using tin and tin oxide gas diffusion electrodes, *J. Appl. Electrochem.*, 2019, **49**, 917–928.

78 Y. Chen, A. Vise, W. E. Klein, F. C. Cetinbas, D. J. Myers, W. A. Smith, W. A. Smith, W. A. Smith, T. G. Deutsch, *et al.*, A Robust, Scalable Platform for the Electrochemical Conversion of CO_2 to Formate: Identifying Pathways to Higher Energy Efficiencies, *ACS Energy Lett.*, 2020, **5**, 1825–1833.

79 J. J. Lv, M. Jouny, W. Luc, W. Zhu, J. J. Zhu and F. Jiao, A Highly Porous Copper Electrocatalyst for Carbon Dioxide Reduction, *Adv. Mater.*, 2018, **30**, 1803111.

80 F. Li, A. Thevenon, A. Rosas-Hernández, Z. Wang, Y. Li, C. M. Gabardo, A. Ozden, C. T. Dinh, J. Li, *et al.*, Molecular tuning of CO_2 -to-ethylene conversion, *Nature*, 2020, **577**, 509–513.

81 W. Ma, S. Xie, T. Liu, Q. Fan, J. Ye, F. Sun, Z. Jiang, Q. Zhang, J. Cheng, *et al.*, Electrocatalytic reduction of CO_2 to ethylene and ethanol through hydrogen-assisted C–C coupling over fluorine-modified copper, *Nat. Catal.*, 2020, **3**, 478–487.

82 M. Zhong, K. Tran, Y. Min, C. Wang, Z. Wang, C. T. Dinh, P. De Luna, Z. Yu, A. S. Rasouli, *et al.*, Accelerated discovery of CO_2 electrocatalysts using active machine learning, *Nature*, 2020, **581**, 178–183.

83 C. M. Gabardo, C. P. O'Brien, J. P. Edwards, C. McCallum, Y. Xu, C. T. Dinh, J. Li, E. H. Sargent and D. Sinton, Continuous Carbon Dioxide Electroreduction to Concentrated Multi-carbon Products Using a Membrane Electrode Assembly, *Joule*, 2019, **3**, 2777–2791.

84 N. Martić, C. Reller, C. Macauley, M. Löffler, B. Schmid, D. Reinisch, E. Volkova, A. Maltenberger, A. Rucki, *et al.*, Paramelaconite-Enriched Copper-Based Material as an Efficient and Robust Catalyst for Electrochemical Carbon Dioxide Reduction, *Adv. Energy Mater.*, 2019, **9**, 1901228.

85 R. Wang, H. Haspel, A. Pustovarenko, A. Dikhtarenko, A. Russkikh, G. Shterk, D. Osadchii, S. Ould-Chikh, M. Ma, *et al.*, Maximizing Ag Utilization in High-Rate CO_2 Electrochemical Reduction with a Coordination Polymer-Mediated Gas Diffusion Electrode, *ACS Energy Lett.*, 2019, **4**, 2024–2031.

86 S. Ma, R. Luo, J. I. Gold, A. Z. Yu, B. Kim and P. J. A. Kenis, Carbon nanotube containing Ag catalyst layers for efficient and selective reduction of carbon dioxide, *J. Mater. Chem. A*, 2016, **4**, 8573–8578.

87 W. Zhu, S. Kattel, F. Jiao and J. G. Chen, Shape-Controlled CO₂ Electrochemical Reduction on Nanosized Pd Hydride Cubes and Octahedra, *Adv. Energy Mater.*, 2019, **9**, 1802840.

88 H. R. Molly Jhong, C. E. Tornow, C. Kim, S. Verma, J. L. Oberst, P. S. Anderson, A. A. Gewirth, T. Fujigaya, N. Nakashima, *et al.*, Gold Nanoparticles on Polymer-Wrapped Carbon Nanotubes: An Efficient and Selective Catalyst for the Electroreduction of CO₂, *ChemPhysChem*, 2017, **18**, 3274–3279.

89 L. Ma, W. Hu, Q. Pan, L. Zou, Z. Zou, K. Wen and H. Yang, Polyvinyl alcohol-modified gold nanoparticles with record-high activity for electrochemical reduction of CO₂ to CO, *J. CO₂ Util.*, 2019, **34**, 108–114.

90 S. Ma, Y. Lan, G. M. J. Perez, S. Moniri and P. J. A. Kenis, Silver Supported on Titania as an Active Catalyst for Electrochemical Carbon Dioxide Reduction, *ChemSusChem*, 2014, **7**, 866–874.

91 Q. Zhu, D. Yang, H. Liu, X. Sun, C. Chen, J. Bi, J. Liu, H. Wu and B. Han, Hollow Metal-Organic-Framework-Mediated In Situ Architecture of Copper Dendrites for Enhanced CO₂ Electroreduction, *Angew. Chem., Int. Ed.*, 2020, **59**, 8896–8901.

92 F. Yang, P. L. Deng, Q. Wang, J. Zhu, Y. Yan, L. Zhou, K. Qi, H. Liu, H. S. Park, *et al.*, Metal-organic framework-derived cupric oxide polycrystalline nanowires for selective carbon dioxide electroreduction to C₂ valuables, *J. Mater. Chem. A*, 2020, **8**, 12418–12423.

93 K. Yao, Y. Xia, J. Li, N. Wang, J. Han, C. Gao, M. Han, G. Shen, Y. Liu, *et al.*, Metal-organic framework derived copper catalysts for CO₂ to ethylene conversion, *J. Mater. Chem. A*, 2020, **8**, 11117–11123.

94 Y. Wang, H. Shen, K. J. T. Livi, D. Raciti, H. Zong, J. Gregg, M. Onadeko, Y. Wan, A. Watson, *et al.*, Copper Nanocubes for CO₂ Reduction in Gas Diffusion Electrodes, *Nano Lett.*, 2019, 8461–8468.

95 W. Ju, F. Jiang, H. Ma, Z. Pan, Y. B. Zhao, F. Pagani, D. Rentsch, J. Wang and C. Battaglia, Electrocatalytic Reduction of Gaseous CO₂ to CO on Sn/Cu-Nanofiber-Based Gas Diffusion Electrodes, *Adv. Energy Mater.*, 2019, **9**, 1901514.

96 H. Xiang, S. Rasul, B. Hou, J. Portoles, P. Cumpson and E. H. Yu, Copper-Indium Binary Catalyst on a Gas Diffusion Electrode for High-Performance CO₂ Electrochemical Reduction with Record CO Production Efficiency, *ACS Appl. Mater. Interfaces*, 2020, **12**, 601–608.

97 K. Ye, Z. Zhou, J. Shao, L. Lin, D. Gao, N. Ta, R. Si, G. Wang and X. Bao, In Situ Reconstruction of a Hierarchical Sn-Cu/SnO_x Core/Shell Catalyst for High-Performance CO₂ Electroreduction, *Angew. Chem., Int. Ed.*, 2020, **59**, 4814–4821.

98 Y. C. Li, Z. Wang, T. Yuan, D. H. Nam, M. Luo, J. Wicks, B. Chen, J. Li, F. Li, *et al.*, Binding Site Diversity Promotes CO₂ Electroreduction to Ethanol, *J. Am. Chem. Soc.*, 2019, **141**, 8584–8591.

99 J. C. Lee, J. Y. Kim, W. H. Joo, D. Hong, S. H. Oh, B. Kim, G. Do Lee, M. Kim, J. Oh, *et al.*, Thermodynamically driven self-formation of copper-embedded nitrogen-doped carbon nanofiber catalysts for a cascade electroreduction of carbon dioxide to ethylene, *J. Mater. Chem. A*, 2020, **8**, 11632–11641.

100 C. Chen, X. Yan, Y. Wu, S. Liu, X. Zhang, X. Sun, Q. Zhu, H. Wu and B. Han, Boosting the Productivity of Electrochemical CO₂ Reduction to Multi-Carbon Products by Enhancing CO₂ Diffusion through a Porous Organic Cage, *Angew. Chem., Int. Ed.*, 2022, **61**, e202202607.

101 C. Chen, X. Yan, S. Liu, Y. Wu, Q. Wan, X. Sun, Q. Zhu, H. Liu, J. Ma, *et al.*, Highly Efficient Electroreduction of CO₂ to C₂+ Alcohols on Heterogeneous Dual Active Sites, *Angew. Chem., Int. Ed.*, 2020, **59**, 16459–16464.

102 C. Yang, H. Shen, A. Guan, J. Liu, T. Li, Y. Ji, A. M. Al-Enizi, L. Zhang, L. Qian, *et al.*, Fast cooling induced grain-boundary-rich copper oxide for electrocatalytic carbon dioxide reduction to ethanol, *J. Colloid Interface Sci.*, 2020, **570**, 375–381.

103 W. Luo, J. Zhang, M. Li and A. Züttel, Boosting CO Production in Electrocatalytic CO₂ Reduction on Highly Porous Zn Catalysts, *ACS Catal.*, 2019, **9**, 3783–3791.

104 F. Y. Gao, S. J. Hu, X. L. Zhang, Y. R. Zheng, H. J. Wang, Z. Z. Niu, P. P. Yang, R. C. Bao, T. Ma, *et al.*, High-Curvature Transition-Metal Chalcogenide Nanostructures with a Pronounced Proximity Effect Enable Fast and Selective CO₂ Electroreduction, *Angew. Chem., Int. Ed.*, 2020, **59**, 8706–8712.

105 A. Löwe, C. Rieg, T. Hierlemann, N. Salas, D. Kopljarić, N. Wagner and E. Klemm, Influence of Temperature on the Performance of Gas Diffusion Electrodes in the CO₂ Reduction Reaction, *ChemElectroChem*, 2019, **6**, 4497–4506.

106 H. Xiang, H. A. Miller, M. Bellini, H. Christensen, K. Scott, S. Rasul and E. H. Yu, Production of formate by CO₂ electrochemical reduction and its application in energy storage, *Sustainable Energy Fuels*, 2019, **4**, 277–284.

107 J. Wang, J. Zou, X. Hu, S. Ning, X. Wang, X. Kang and S. Chen, Heterostructured intermetallic CuSn catalysts: high performance towards the electrochemical reduction of CO₂ to formate, *J. Mater. Chem. A*, 2019, **7**, 27514–27521.

108 G. Díaz-Sainz, M. Alvarez-Guerra, J. Solla-Gullón, L. García-Cruz, V. Montiel and A. Irabien, CO₂ electroreduction to formate: Continuous single-pass operation in a filter-press reactor at high current densities using Bi gas diffusion electrodes, *J. CO₂ Util.*, 2019, **34**, 12–19.

109 P. Deng, F. Yang, Z. Wang, S. Chen, Y. Zhou, S. Zaman and B. Y. Xia, Metal-Organic Framework-Derived Carbon Nanorods Encapsulating Bismuth Oxides for Rapid and Selective CO₂ Electroreduction to Formate, *Angew. Chem., Int. Ed.*, 2020, **59**, 10807–10813.

110 J. Yang, X. Wang, Y. Qu, X. Wang, H. Huo, Q. Fan, J. Wang, L. M. Yang and Y. Wu, Bi-Based Metal-Organic

Framework Derived Leafy Bismuth Nanosheets for Carbon Dioxide Electroreduction, *Adv. Energy Mater.*, 2020, **10**, 2001709.

111 C. Cao, D. D. Ma, J. F. Gu, X. Xie, G. Zeng, X. Li, S. G. Han, Q. L. Zhu, X. T. Wu, *et al.*, Metal-Organic Layers Leading to Atomically Thin Bismuthene for Efficient Carbon Dioxide Electroreduction to Liquid Fuel, *Angew. Chem., Int. Ed.*, 2020, **59**, 15014–15020.

112 H. Yang, Y. Wu, Q. Lin, L. Fan, X. Chai, Q. Zhang, J. Liu, C. He and Z. Lin, Composition Tailoring via N and S Co-doping and Structure Tuning by Constructing Hierarchical Pores: Metal-Free Catalysts for High-Performance Electrochemical Reduction of CO₂, *Angew. Chem., Int. Ed.*, 2018, **57**, 15476–15480.

113 C. Chen, X. Sun, X. Yan, Y. Wu, H. Liu, Q. Zhu, B. B. A. Bediako and B. Han, Boosting CO₂ Electroreduction on N,P-Co-doped Carbon Aerogels, *Angew. Chem., Int. Ed.*, 2020, **59**, 11123–11129.

114 H. Yang, Q. Lin, C. Zhang, X. Yu, Z. Cheng, G. Li, Q. Hu, X. Ren, Q. Zhang, *et al.*, Carbon dioxide electroreduction on single-atom nickel decorated carbon membranes with industry compatible current densities, *Nat. Commun.*, 2020, **11**, 1–8.

115 H. Yang, Q. Lin, Y. Wu, G. Li, Q. Hu, X. Chai, X. Ren, Q. Zhang, J. Liu, *et al.*, Highly efficient utilization of single atoms via constructing 3D and free-standing electrodes for CO₂ reduction with ultrahigh current density, *Nano Energy*, 2020, **70**, 104454.

116 J. Gu, C. S. Hsu, L. Bai, H. M. Chen and X. Hu, Atomically dispersed Fe³⁺ sites catalyze efficient CO₂ electroreduction to CO, *Science*, 2019, **364**, 1091–1094.

117 H. Y. Jeong, M. Balamurugan, V. S. K. Choutipalli, E. S. Jeong, V. Subramanian, U. Sim and K. T. Nam, Achieving highly efficient CO₂ to CO electroreduction exceeding 300 mA cm⁻² with single-atom nickel electrocatalysts, *J. Mater. Chem. A*, 2019, **7**, 10651–10661.

118 Y. Wang, Z. Jiang, X. Zhang, Z. Niu, Q. Zhou, X. Wang, H. Li, Z. Lin, H. Zheng, *et al.*, Metal Phthalocyanine-Derived Single-Atom Catalysts for Selective CO₂ Electroreduction under High Current Densities, *ACS Appl. Mater. Interfaces*, 2020, **12**, 33795–33802.

119 X. Zhang, Y. Wang, M. Gu, M. Wang, Z. Zhang, W. Pan, Z. Jiang, H. Zheng, M. Lucero, *et al.*, Molecular engineering of dispersed nickel phthalocyanines on carbon nanotubes for selective CO₂ reduction, *Nat. Energy*, 2020, **5**, 684–692.

120 C. F. Wen, F. Mao, Y. Liu, X. Y. Zhang, H. Q. Fu, L. R. Zheng, P. F. Liu and H. G. Yang, Nitrogen-Stabilized Low-Valent Ni Motifs for Efficient CO₂ Electrocatalysis, *ACS Catal.*, 2020, **10**, 1086–1093.

121 M. Wang, K. Torbensen, D. Salvatore, S. Ren, D. Joulié, F. Dumoulin, D. Mendoza, B. Lassalle-Kaiser, U. Işçi, *et al.*, CO₂ electrochemical catalytic reduction with a highly active cobalt phthalocyanine, *Nat. Commun.*, 2019, **10**, 1–8.

122 K. Chen, M. Cao, Y. Lin, J. Fu, H. Liao, Y. Zhou, H. Li, X. Qiu, J. Hu, *et al.*, Ligand Engineering in Nickel Phthalocyanine to Boost the Electrocatalytic Reduction of CO₂, *Adv. Funct. Mater.*, 2022, **32**, 2111322.

123 K. Torbensen, C. Han, B. Boudy, N. von Wolff, C. Bertail, W. Braun and M. Robert, Iron Porphyrin Allows Fast and Selective Electrocatalytic Conversion of CO₂ to CO in a Flow Cell, *Chem. – Eur. J.*, 2020, **26**, 3034–3038.

124 K. Xie, R. K. Miao, A. Ozden, S. Liu, Z. Chen, C. T. Dinh, J. E. Huang, Q. Xu, C. M. Gabardo, *et al.*, Bipolar membrane electrolyzers enable high single-pass CO₂ electroreduction to mult carbon products, *Nat. Commun.*, 2022, **13**, 1–12.

125 S. Li, W. Chen, X. Dong, C. Zhu, A. Chen, Y. Song, G. Li, W. Wei and Y. Sun, Hierarchical micro/nanostructured silver hollow fiber boosts electroreduction of carbon dioxide, *Nat. Commun.*, 2022, **13**, 1–9.

126 Y. Wang, Z. Wang, C. T. Dinh, J. Li, A. Ozden, M. Golam Kibria, A. Seifitokaldani, C. S. Tan, C. M. Gabardo, *et al.*, Catalyst synthesis under CO₂ electroreduction favours faceting and promotes renewable fuels electrosynthesis, *Nat. Catal.*, 2019, **3**, 98–106.

127 T. Zhang, J. C. Bui, Z. Li, A. T. Bell, A. Z. Weber and J. Wu, Highly selective and productive reduction of carbon dioxide to mult carbon products via in situ CO management using segmented tandem electrodes, *Nat. Catal.*, 2022, **5**, 202–211.

128 J. H. Guo, X. Y. Zhang, X. Y. Dao and W. Y. Sun, Nanoporous Metal–Organic Framework-Based Ellipsoidal Nanoparticles for the Catalytic Electroreduction of CO₂, *ACS Appl. Nano Mater.*, 2020, **3**, 2625–2635.

129 J. R. Huang, X. F. Qiu, Z. H. Zhao, H. L. Zhu, Y. C. Liu, W. Shi, P. Q. Liao and X. M. Chen, Single-Product Faradaic Efficiency for Electrocatalytic of CO₂ to CO at Current Density Larger than 1.2 A cm⁻² in Neutral Aqueous Solution by a Single-Atom Nanozyme, *Angew. Chem., Int. Ed.*, 2022, **61**, e202210985.

130 B. Endrdi, E. Kecsenovity, A. Samu, T. Halmágyi, S. Rojas-Carbonell, L. Wang, Y. Yan and C. Janáky, High carbonate ion conductance of a robust PiperION membrane allows industrial current density and conversion in a zero-gap carbon dioxide electrolyzer cell, *Energy Environ. Sci.*, 2020, **13**, 4098–4105.

131 N. Fujinuma, A. Ikoma and S. E. Lofland, Highly Efficient Electrochemical CO₂ Reduction Reaction to CO with One-Pot Synthesized Co-Pyridine-Derived Catalyst Incorporated in a Nafion-Based Membrane Electrode Assembly, *Adv. Energy Mater.*, 2020, **10**, 2001645.

132 J. A. Rabinowitz and M. W. Kanan, The future of low-temperature carbon dioxide electrolysis depends on solving one basic problem, *Nat. Commun.*, 2020, **11**, 1–3.

133 M. Ma, E. L. Clark, K. T. Therkildsen, S. Dalsgaard, I. Chorkendorff and B. Seger, Insights into the carbon balance for CO₂ electroreduction on Cu using gas diffusion electrode reactor designs, *Energy Environ. Sci.*, 2020, **13**, 977–985.

134 E. R. Cofell, U. O. Nwabara, S. S. Bhargava, D. E. Henckel and P. J. A. Kenis, Investigation of Electrolyte-Dependent Carbonate Formation on Gas Diffusion Electrodes for CO₂

Electrolysis, *ACS Appl. Mater. Interfaces*, 2021, **13**, 15132–15142.

135 C. P. O'Brien, R. K. Miao, S. Liu, Y. Xu, G. Lee, A. Robb, J. E. Huang, K. Xie, K. Bertens, *et al.*, Single Pass CO₂ Conversion Exceeding 85% in the Electrosynthesis of Multicarbon Products via Local CO₂ Regeneration, *ACS Energy Lett.*, 2021, **6**, 2952–2959.

136 B. Pan, J. Fan, J. Zhang, Y. Luo, C. Shen, C. Wang, Y. Wang and Y. Li, Close to 90% Single-Pass Conversion Efficiency for CO₂ Electroreduction in an Acid-Fed Membrane Electrode Assembly, *ACS Energy Lett.*, 2022, **7**, 4224–4231.

137 J. Disch, L. Bohn, S. Koch, M. Schulz, Y. Han, A. Tengattini, L. Helfen, M. Breitwieser and S. Vierrath, High-resolution neutron imaging of salt precipitation and water transport in zero-gap CO₂ electrolysis, *Nat. Commun.*, 2022, **13**, 1–9.

138 S. Garg, Q. Xu, A. B. Moss, M. Mirolo, W. Deng, I. Chorkendorff, J. Drnec and B. Seger, How alkali cations affect salt precipitation and CO₂ electrolysis performance in membrane electrode assembly electrolyzers, *Energy Environ. Sci.*, 2023, **16**, 1631–1643.

139 R. Krause, D. Reinisch, C. Reller, H. Eckert, D. Hartmann, D. Taroata, K. Wiesner-Fleischer, A. Bulan, A. Lueken, *et al.*, Industrial Application Aspects of the Electrochemical Reduction of CO₂ to CO in Aqueous Electrolyte, *Chem. Ing. Tech.*, 2020, **92**, 53–61.

140 J. Timoshenko, A. Bergmann, C. Rettenmaier, A. Herzog, R. M. Arán-Ais, H. S. Jeon, F. T. Haase, U. Hejral, P. Grosse, *et al.*, Steering the structure and selectivity of CO₂ electroreduction catalysts by potential pulses, *Nat. Catal.*, 2022, **5**, 259–267.

141 S. Liu, H. Tao, L. Zeng, Q. Liu, Z. Xu, Q. Liu and J. L. Luo, Shape-Dependent Electrocatalytic Reduction of CO₂ to CO on Triangular Silver Nanoplates, *J. Am. Chem. Soc.*, 2017, **139**, 2160–2163.

142 Y. Zhu, Z. Gao, Z. Zhang, T. Lin, Q. Zhang, H. Liu, L. Gu and W. Hu, Selectivity regulation of CO₂ electroreduction on asymmetric AuAgCu tandem heterostructures, *Nano Res.*, 2022, **15**, 7861–7867.